

Thermonuclear X-ray Bursts: Theory vs. Observations

Andrew Cumming^a

^aHubble Fellow, Department of Astronomy and Astrophysics, University of California, Santa Cruz;
cumming@ucolick.org

I review our theoretical understanding of thermonuclear flashes on accreting neutron stars, concentrating on comparisons to observations. Sequences of regular Type IX-ray bursts from GS 1826-24 and 4U 1820-30 are very well described by the theory. I discuss recent work which attempts to use the observed burst properties in these sources to constrain the composition of the accreted material. For GS 1826-24, variations in \dot{m} with accretion rate indicate that the accreted material has solar metallicity; for 4U 1820-30, future observations should constrain the hydrogen fraction, testing evolutionary models. I briefly discuss the global bursting behavior of burst sources, which continues to be a major puzzle. Finally, I turn to superbursts, which naturally fit into the picture as unstable carbon ignition in a thick layer of heavy elements. I present new time-dependent models of the cooling tails of superbursts, and discuss the various interactions between superbursts and normal Type I bursts, and what can be learned from them.

1. INTRODUCTION

Type I X-ray bursts were discovered in the 1970's, and quickly understood as being due to unstable burning of hydrogen and helium on the surface of an accreting neutron star (for reviews see [34,48]). Fuel accumulates for hours to days, and then ignites and burns in a ~ 10 – 100 s burst with typical energy $\sim 10^{39}$ – 10^{40} ergs.

In recent years, there has been a lot of excitement in the field. First, the Rossi X-Ray Timing Explorer (RXTE) discovered nearly-coherent oscillations during bursts, with frequencies in the range 270–620 Hz [48]. Believed to be rotationally-modulated brightness asymmetries on the neutron star surface, the oscillation frequency tells us the neutron star spin, and potentially about the spreading of burning, and the surface magnetic field [9].

Second, long term monitoring of bursters with BeppoSAX/WFC (Verbunt, this volume) and RXTE/ASM and PCA has revealed a new class of rare, extremely energetic, and long duration bursts now known as "superbursts" ([30]; Kuulkers, this volume), as well as a new class of low luminosity burst sources discovered through their burst rather than persistent emission ([13]; Corneisse, this volume). Particularly important has

been the large amount of data accumulated on bursters by the Wide Field Camera (WFC) survey of the Galactic center, which has also enlarged our sample of normal Type I bursts [14].

In this article, I review our theoretical understanding of thermonuclear flashes on accreting neutron stars, concentrating on how well it compares to observations, and what we can learn from such a comparison.

2. HOW THE ACCRETED HYDROGEN AND HELIUM BURNS

The physics of nuclear burning on the surface of an accreting neutron star has been discussed by many authors, comprehensive reviews can be found in refs. [34,4,48]. Here I briefly review how the accreted hydrogen and helium burns, and the expected burst properties as a function of accretion rate. In particular, I concentrate on the differences between hydrogen and helium burning, which are crucial for understanding the regimes of burning, and for comparing to observations.

The timescale for burning τ whereas helium burning proceeds rapidly via strong interactions, hydrogen burning is relatively slow, since beta decays are required to convert protons to neutrons. This leads to a saturation of the CNO

burning rate at high temperatures $T \approx 8 \cdot 10^7$ K (the so-called "hot CNO cycle"; [29]), when proton captures in the cycle occur more rapidly than the subsequent beta-decays. At high accretion rates, hot CNO burning during accumulation of fuel depletes hydrogen prior to the runaway. The time to burn all the hydrogen in a given fluid element is

$$t_H = 11 \text{ hrs} \frac{0.02}{Z} \frac{X_0}{0.7}; \quad (1)$$

where Z is the CNO mass fraction.

The amount of hydrogen vs. helium present at ignition of the burst has a direct impact on the burst lightcurve. If the helium fraction is large, the rapid energy release at the beginning of the burst creates a luminosity exceeding the Eddington luminosity, driving outwards expansion of the photosphere ("photospheric radius expansion") [22]. If hydrogen dominates the composition however, it burns after ignition via the rp-process [57,42]. Starting with seed nuclei made by helium burning, this comprises a series of proton captures and beta-decays involving nuclei close to the proton drip line and extending well beyond the iron group. This can significantly delay the cooling of the burning layer, giving an extended burst tail, and burst durations ≈ 100 s [27,60].

Thermal stability | The nature of the instability is a thin shell flash [28], in which temperature perturbations drive runaway heating through temperature sensitive nuclear reactions. Hot CNO hydrogen burning is thermally stable, since the burning rate does not respond to temperature fluctuations. However, at the lowest accretion rates $\dot{M} \approx 0.01 \dot{M}_{\text{Edd}}$, $T < 8 \cdot 10^7$ K in the accumulating layer and the usual CNO cycle operates, allowing unstable hydrogen ignition and leading to "hydrogen-triggered" bursts. For $\dot{M} \approx 0.01 \dot{M}_{\text{Edd}}$, the hydrogen burns stably, and helium burning at a density $\approx 10^5 \text{ g cm}^{-3}$ drives the thermal instability.

Helium triggered bursts are of two types, depending on the time to accumulate the critical

¹depending on metallicity, see [4] for the scalings. I take $\dot{M}_{\text{Edd}} = 1.7 \cdot 10^8 \text{ M}_{\odot} \text{ yr}^{-1}$, the Eddington accretion rate for a 10 km neutron star accreting solar composition material.

column of fuel (or equivalently the recurrence time of the bursts t_{recur}). If $t_{\text{recur}} > t_H$, hydrogen burns away and ignition occurs in a pure helium layer below a steady burning hydrogen shell, giving a "pure He" burst; if $t_{\text{recur}} < t_H$, hydrogen is present throughout the layer when the helium ignites, giving a "mixed H/He" burst.

For $\dot{M} \approx \dot{M}_{\text{Edd}}$, helium burns at a temperature $T \approx 5 \cdot 10^8$ K for which the temperature sensitivity of the triple alpha reaction is less than the temperature sensitivity of the cooling. The burning is then thermally stable, and the fuel burns at the rate it accretes. The accretion rate at which burning stabilizes and its dependence on metallicity is still not well-determined theoretically.

Nuclear energy release | hydrogen burning releases substantially more energy per gram, $Q_{\text{nuc}} \approx 7 \text{ MeV}$ per nucleon compared to only 1.6 MeV per nucleon from helium burning. Observationally, the energy release per gram is measured by the parameter β , the ratio of persistent flux between bursts to burst flux,

$$\beta = \frac{\int_0^t F_p dt}{\int_0^t F_b dt} = \frac{(GM = R)}{Q_{\text{nuc}}}; \quad (2)$$

where F_p is the persistent flux from accretion, F_b is the burst flux, t is the interval from the beginning of one burst to the next, and $GM = R \approx 200 \text{ MeV}$ per nucleon is the gravitational energy release. We expect $\beta \approx 40$ if the material burned in the burst is solar composition, compared to ≈ 100 for pure helium. (These numbers are somewhat uncertain given that not all of the accretion energy necessarily appears in X-rays, and the X-ray emission is potentially anisotropic). Measurement of β values in the expected range was an important initial confirmation of the thermal nuclear flash model for Type I bursts.

The large energy release from hydrogen burning plays an important role in setting the conditions for ignition of the flash. Figure 1 shows illustrative temperature profiles as a function of column depth (g cm^{-2}) into the star at the moment of ignition for each of the four different burning regimes for the case of solar metallicity. The dashed and dotted curves are ignition curves for hydrogen and helium, calculated using a local ap-

proximation for the cooling rate following ref. [16] (I refer to that paper for details, also see [37] for recent calculations of the global eigenfunctions).

In the mixed H/He burst regime for solar metallicity, the ignition conditions are well-determined, since the temperature profile is set by hot CNO burning within the accumulating layer. The ignition column depth is $(1-2) \cdot 10^8 \text{ g cm}^{-2}$, roughly independent of accretion rate, so that bursts in this regime are expected to have constant energy, and a recurrence time which scales close to \dot{M}^{-1} .

For low metallicity mixed H/He bursts, pure He bursts, and hydrogen-triggered bursts, the internal heating from hot CNO burning is either much less or absent altogether. The temperature profile is then set by compressional heating or heating from below, either heat from reactions occurring deep in the neutron star crust [6], or residual heat from burning of leftover fuel in the ashes of a previous burst [51,60]. The ignition conditions are therefore sensitive to accretion rate, and might be expected to show variations from burst to burst (i.e. less regular bursting). This is particularly true for pure He bursts because of the very shallow slope of the ignition temperature with column depth.

3. COMPARISON WITH OBSERVATIONS

3.1. Regular bursting I: GS 1826-24, The "Locked Burster"

The transient source GS 1826-24 was discovered by Ginga, and regularly monitored by BeppoSAX, which revealed it to be an extremely regular Type I burster. Ubertini et al. [53], who dubbed this source the "locked" burster, found the burst recurrence time was close to 6 hours with a dispersion of only 6 minutes. Further monitoring showed that the recurrence time decreased as the source brightened [14].

Based on the energetics and recurrence times, as well as the long duration of the bursts, Bildsten [5] proposed that this was a textbook case of mixed H/He bursting. This is the expected burning regime at the inferred accretion rate of $0.1 \dot{M}_{\text{Edd}}$ and observed recurrence times of < 6

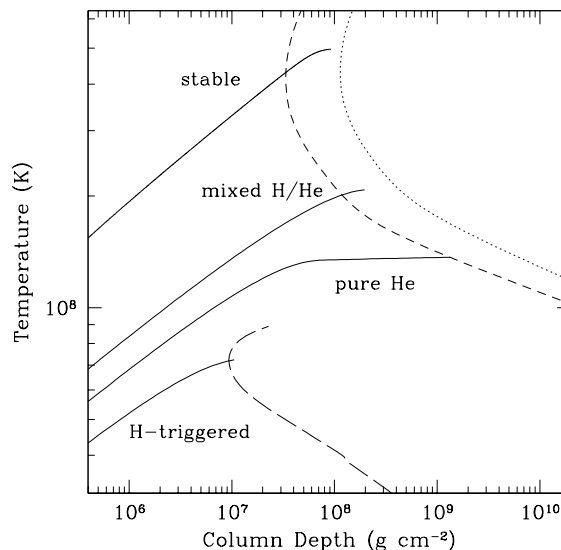


Figure 1. Illustrative temperature profiles (solid curves) in the different burning regimes, for solar metallicity. The dotted and short-dashed lines are helium ignition curves (helium mass fraction $Y = 0.3$ and $Y = 1.0$ respectively); the long-dashed line is the hydrogen ignition curve.

hours, and is consistent with the measured $\dot{M} = 40-60$. In addition, the inferred ignition mass is as expected from theory. The burst energy of $5 \cdot 10^{39} \text{ erg}$ implies an ignition mass of 10^{21} g for a nuclear energy release $5 \cdot 10^{18} \text{ erg g}^{-1}$ (equivalently, this is the mass accreted in a recurrence time at the observed \dot{M}). The corresponding column depth is $y_{\text{ign}} \approx 10^8 \text{ g cm}^{-2}$, exactly as expected for mixed H/He ignition with solar metallicity ($Z = 0.02$) (Figure 1; see also Table 2 of [16]).

Given the excellent agreement with theory, a natural question is whether we can use the bursts to constrain properties of the source [24]. For mixed H/He bursts, the ignition depth is mainly sensitive to the metallicity, because the temperature profile of the accumulating layer is set by hot CNO burning. This suggests an argument to constrain the metallicity: if it was less than solar, the reduced CNO heating would give a larger

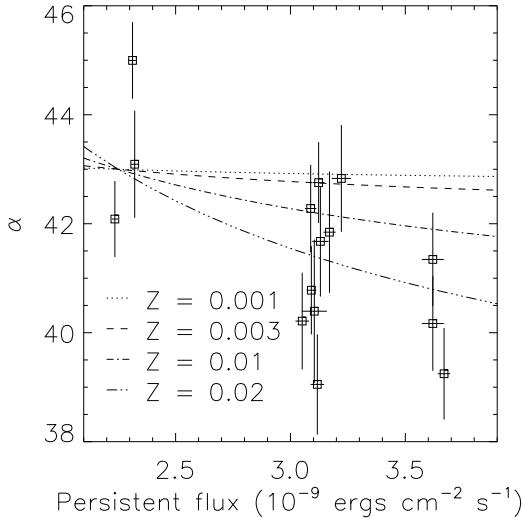


Figure 2. Ratio of persistent to burst luminosity $= L_p/L_b$ (equation 2), calculated from RXTE observations between 1997 and 2002. Error bars represent the estimated 1 σ uncertainties. From Galloway et al. (2003) (ref.[24]). The changing α with M_{bol} indicates that fuel is burning between bursts, as expected for hot CNO hydrogen burning with solar metallicity.

ignition column depth, and a larger recurrence time and burst energy than observed. However, the uncertainty in the relation between M_{bol} and the X-ray luminosity L_x allows lower metallicity models to be accommodated by adopting a larger M_{bol} (the larger column is then accreted in the observed recurrence time)². Additionally, the time-dependent simulations of Woosley et al. [60] show that at low metallicity, a new heat source takes over. Production of CNO elements in the tail of the previous X-ray burst leads to leftover hydrogen burning beneath the newly accreted layer ("compositional inertia"), reducing the sensitivity to metallicity (see also [27]).

Determining the metallicity requires an additional constraint on the models. Galloway et al. [24] recently concluded that the metallicity in

²In fact, the best approach is to turn this around: given a metallicity, we "measure" the local accretion rate onto the star by matching the observed recurrence time.

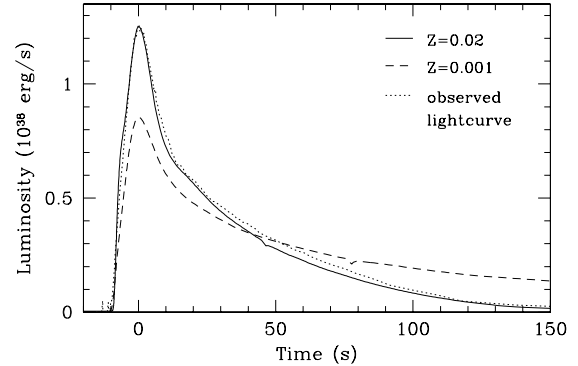


Figure 3. The average observed lightcurve from GS 1826-24 (dotted line; ref. [24]) compared with theoretical simulations (solid and dashed lines; models ZM and zM of ref. [60]). The observed and theoretical recurrence times are both ≈ 4 hours.

the accreted layer was solar by looking at variations of burst properties with M_{bol} . They present data for 24 bursts observed by RXTE between 1997 and 2002. The α value was found to decrease by 10% as accretion rate increased by 50% (Figure 2). This is exactly as expected from models with solar metallicity [16], since as accretion rate increases and recurrence time drops, less time is available to burn hydrogen between bursts. Models with metallicity much less than solar are hard to reconcile with the variations.

Another constraint comes from the burst lightcurves, which show a long ≈ 10 s rise and a long ≈ 100 s tail³. Theoretical models of mixed H/He bursts (e.g. [27,43]) show long burst tails, leading Bildsten [4] to argue that an active rp-process powers the bursts from GS 1826-24. Figure 3 compares the average observed burst lightcurve with the recent simulations of Woosley et al. [60]. These simulations are the first to incorporate a large nuclear reaction network that can follow the detailed rp process nucleosynthesis together with resolved vertical structure. The

³The burst lightcurves were remarkably similar during this period, with only a small variation as M_{bol} increased with time. This, together with the extremely regular nature of the burning, argues for complete burning of the fuel in each burst, and complete covering of the stellar surface.

agreement between the observed lightcurve and solar metallicity model is remarkable, supporting the findings of Galloway et al. [24]. A more detailed comparison with the simulations is in progress. The predicted burst lightcurves are sensitive to the nuclear physics input [60], and so there is potentially much to learn.

The ignition column for mixed H/He bursts is predicted to be roughly independent of accretion rate, since hot CNO burning sets the temperature in the accreted layer (x2). Galloway et al. [24] find that $t_{\text{recur}} / M^{-1.05 \pm 0.02}$, implying a slight decrease in the ignition column with M , $\gamma_{\text{ign}} / M^{-0.05}$. This remains to be understood; a simple argument suggests a slight increase should be seen, since less helium is produced by hot CNO burning for a shorter recurrence time, requiring a slightly thicker layer to ignite. Two possible explanations for the discrepancy are (i) extra heating, e.g. from thermal or compositional inertia effects [51,60], or (ii) the fraction of the star covered by fuel changes with M . Future comparisons with time-dependent simulations or improved spectral models should test these ideas.

3.2. Regular bursting II: 4U 1820-30

The ultracompact binary 4U 1820-30 (orbital period 11.4 mins [47]) is an interesting source in which to study Type I bursting behaviour. It has a known distance, being located in the metal-rich globular cluster NGC 6624 ($[Fe/H] = 0.4$, distance 7.6 ± 0.4 kpc) [32]. It undergoes a characteristic 176 day accretion cycle [40] during which the accretion rate varies by a factor of 3 or more. Regular sequences of Type I bursts are observed during the low state, with recurrence times of $\sim 2\text{--}4$ hours [11,12,26,14]. In the high state, bursts become irregular or disappear altogether [10,14]. This source also showed the most energetic and luminous superburst [49].

The extremely short orbital period implies a hydrogen-deficient companion, and observations of bursts support this picture, with ~ 120 [26] as expected for helium rich material. Different evolutionary models predict that the accreted matter is either pure helium [55,1,41], or contains a small amount of hydrogen (perhaps 5–35% by mass; [52,19,39]). Recently, I looked at

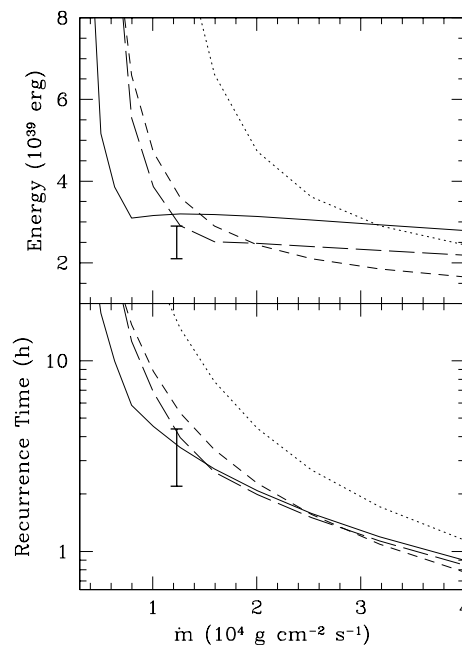


Figure 4. Predicted burst energy and recurrence time as a function of assumed local accretion rate \dot{m} for 4U 1820-30 (ref. [15]). Choosing \dot{m} allows both pure helium models (dotted and short-dashed lines) and models with hydrogen (long-dashed line 10% hydrogen; solid line 20% hydrogen) to fit the observed values (indicated by error bars and placed at the value of \dot{m} inferred from the X-ray luminosity).

the question of whether the composition of the accreted material (especially the hydrogen fraction) might be inferred from the burst properties [15]. This is important to test intermediate-mass binary evolution models for X-ray binaries (e.g. [39]) which predict a small amount of hydrogen may be present.

The inferred accretion rate when bursts are seen from 4U 1820-30 is $\dot{M} = 2.4 \times 10^{-9} M_{\odot} \text{ yr}^{-1}$, giving an ignition column depth $\sim 2 \times 10^8 \text{ g cm}^{-2}$. Bildsten [3] found that this compares well with time-dependent models of pure helium burning, although for a slightly hotter base temperature than expected. The reason for this can be seen by inspecting Figure 1. Ignition at $\gamma = 10^8 \text{ g cm}^{-2}$

requires heating equivalent to hot CNO burning with $Z = 0.01$. In the pure helium case, this heating must be provided by a heat flux into the layer from below, and translates to a flux equivalent to 0.4 M eV per accreted nucleon, higher than the expected crust luminosity [6].

If hydrogen is present with mass fraction $X = 0.1$, hot CNO burning during accumulation could provide the required heating [15] (this requires $Z \approx 3 \times 10^{-3}$, likely satisfied for 4U 1820-30). This is illustrated in Figure 4, which shows the predicted recurrence times and burst energies for models with and without hydrogen, compared to observed values. Models with hydrogen do much better for the accretion rate inferred from the X-ray luminosity. However, it is not possible to reach a firm conclusion because increasing the accretion rate by only a factor of two allows pure helium models to come into agreement.

As for GS 1826-24, an additional constraint is required to determine the accreted composition. One possibility is to look for variations of the burst energetics with accretion rate. For 10% accreted hydrogen, the time to burn all the hydrogen is 3 hours, comparable to the recurrence time. This leads to 10% variations in burst energy as recurrence time varies. This is a promising way to constrain the accreted composition, but will require further observations of sequences of regular bursting with different recurrence times. Another possible constraint comes from simultaneous modelling of Type I bursts and superbursts, I discuss this further in §4.3. It would also be interesting to compare burst lightcurves with time-dependent simulations.

3.3. Global bursting behaviour

The properties of regular burst sequences from both GS 1826-24 and 4U 1820-30 agree very well with theoretical expectations, and we have discussed to what extent we can learn about the accreted composition in these cases. However, it has been pointed out many times that the global bursting behavior is not understood, and for many bursters is opposite to that predicted by theory [56,5]. EXOSAT observations of several A-toll sources showed that as X-ray luminosity increased, burst properties changed from reg-

ular, frequent bursts ($t_{\text{recur}} \sim \text{hours}$) with long durations ($\sim 30 \text{ s}$) and low $\dot{M} \sim 40$, to irregular, infrequent ($t_{\text{recur}} > 1 \text{ day}$), short ($< 10 \text{ s}$) bursts with high $\dot{M} > 100$ and often showing photospheric radius expansion (PRE) (e.g. [56]). RXTE and BeppoSAX observations have confirmed this result, with particularly good coverage for the transient source KS 1731-260 [35,14]. Comelisse et al. [14] found that observations of nine bursters were consistent with this pattern of bursting, with a universal transition luminosity $L_X \approx 2 \times 10^{37} \text{ erg s}^{-1}$ (although not all showed the transition from one burst type to another).

The short bursts are naturally interpreted as pure He bursts; the long bursts as mixed H/He bursts⁴. However, theory predicts a transition from pure He bursts to mixed H/He bursts as accretion rate increases rather than the other way around (x2). Several explanations have been proposed, all of which require further investigation. In the context of 1D models, mixing of fuel by Rayleigh-Taylor [58] or shear instabilities [22] might allow more rapid burning of hydrogen; Woosley et al. [60] have again emphasised the importance of "compositional inertia", that bursts ignite on the ashes of previous bursts; Narayan & Heyl [37] calculate linear models of steady burning models, and find fuel is burned before the runaway. Bildsten has stressed that solving this puzzle may require going beyond spherical symmetry, understanding both the burning front propagation [3], and the fuel covering fraction [4].

Some relevant observational facts are (i) regular bursting seen in GS 1826 is well-understood as mixed H/He bursts, arguing that other bursters such as KS 1731-260 are in this burning regime when regular bursting is seen — if so (unless changes in covering fraction reverse the local ac-

⁴Note that classifying short bursts as "helium" and long bursts as "hydrogen" is appropriate for bursts with similar ignition column depths, but care should be taken when looking at bursts from a wide range of accretion rates. For example, at low accretion rates, the opposite behavior may be true, with long, energetic pure helium bursts and short hydrogen-triggered bursts. The best quantity to distinguish the composition is \dot{M} . The lightcurves of a long mixed H/He burst and long pure He burst will also look very different; e.g. the latter will most likely show a large photospheric radius expansion episode.

cretion rate trend [4]), as \dot{M} drops to the point where the recurrence time is t_{H} or longer, a transition at low \dot{M} into pure helium bursts should be observed; (ii) large values ~ 1000 are often seen at high \dot{M} , implying that both H and He are burning outside bursts; (iii) 4U 1820-30 has a similar luminosity at which regular bursting stops | if the same mechanism applies, it must be composition-independent.

Other sources show different behavior. In particular, SAS-3 [2] and later RXTE [20,54] observations show that bursts from 4U 1728-34 have helium-like characteristics (~ 110 and durations ~ 10 s), but become less energetic, stop showing PRE, and occur more often as accretion rate increases. The burst uence is proportional to the recurrence time; very different to the constant uence expected for mixed H/He burning. Detailed models of the bursts from this source have not been made, but the observations perhaps suggest accretion of He-rich material, with very little H burning between bursts.

The difference in bursting behavior is correlated with the spin frequency measured during Type I bursts. KS 1731-260 [35] has $\nu_{\text{spin}} = 524$ Hz; 4U 1728-34 [20,54] has $\nu_{\text{spin}} = 363$ Hz. For both sources, burst oscillations are seen in the high accretion rate state only: for KS 1731-260, this is mostly for PRE bursts; for 4U 1728-34, this is mostly for bursts without PRE. Munro and coworkers have shown that the correlation of the presence of burst oscillations with or without PRE applies to other sources with spins ~ 600 Hz or ~ 300 Hz respectively [36]. This suggests that a detailed analysis of burst properties would show that bursters with ~ 300 Hz spins are similar to 4U 1728-34, and those with ~ 600 Hz are similar to KS 1731-260. It is not clear what this is telling us, perhaps that the two groups of systems have different evolutionary histories, and hence accreted compositions and burst properties.

4. SUPERBURSTS

4.1. Superbursts as carbon ashes

A summary of observations of superbursts is given by Kuulkers, this volume (see also refs. [30], [48]). Basic energetic arguments point to igni-

tion of a layer of fuel much more massive than a typical Type I burst. For a nuclear energy release of 1 MeV per nucleon, 10^{24} g is needed to match the observed superburst energy of 10^{42} ergs. At an accretion rate $\sim 0.1 \dot{M}_{\text{Edd}}$ appropriate for these sources, this mass is accreted in a few months. Since helium ignites at much lower masses at these \dot{M} 's (and indeed these sources show ordinary Type I bursts), the superbursts require a new fuel. Theoretical attention has focused on carbon, which calculations show is present in the ashes of H/He burning, e.g. [8,46].

Carbon ignition on accreting neutron stars was studied by several authors in the 1970's [61,50,33] (originally as a gamma-ray burst model), and more recently for rapidly accreting neutron stars ($\dot{M} > \dot{M}_{\text{Edd}}$) by Brown and Bildsten [8]. These calculations found ignition masses of 10^{26} g, giving characteristic energies 10^{43} (10^{44} ergs, and recurrence times 10 (100 years at $0.1 \dot{M}_{\text{Edd}}$). Therefore carbon ashes initially appeared too energetic to match the 10^{42} erg superbursts and probably too rare to match the number discovered (the superburst recurrence time is not well-constrained, but was at most ~ 6 years in one source [59]).

However, two pieces of physics act to reduce the observed energies and recurrence times. Strohmayer & Brown [49] modeled the superburst in 4U 1820-30 as ignition of a 10^{26} g layer with 30% carbon and 70% iron by mass. Because this source accretes helium-rich matter, stable burning is able to produce large amounts of carbon [8]. At the peak temperature of the ash ($> 5 \times 10^9$ K), neutrino emission is very efficient and Strohmayer & Brown found that 90% of the energy was lost as neutrinos, leaving 10^{42} erg to be radiated from the surface in the first few hours.

The other superburst sources accrete hydrogen and helium, in which case protons readily capture on carbon during hydrogen/helium burning. The amount of carbon produced is small, 10% for stable burning, or $\sim 1\%$ for unstable burning [46]. However, Cumming & Bildsten [17] showed that even a small amount of carbon is enough to power a superburst. The key physics is that the heavy elements that make up most of the mix-

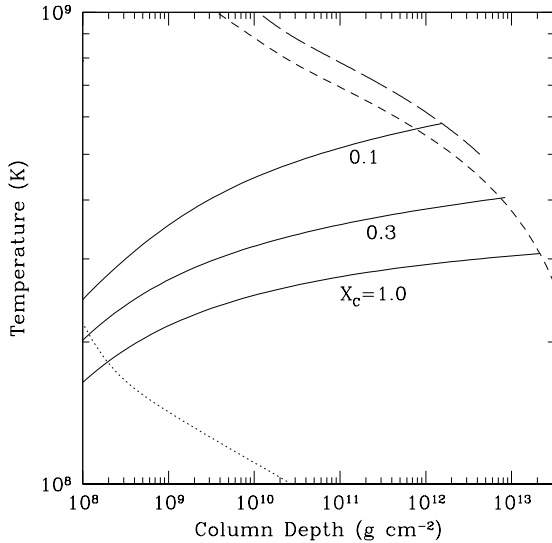


Figure 5. Temperature profiles in the carbon/heavy element layer (solid lines) for different carbon mass fractions. The short and long dashed lines show carbon ignition curves for $X_c = 1.0$ and 0.1 ; the dotted line shows the pure helium triple alpha ignition curve for comparison.

ture have a low thermal conductivity (this is especially true for the very heavy nuclei made in the rp-process). This makes a steeper temperature gradient, leading to ignition at a factor ~ 10 lower in column depth. This is illustrated in Figure 5, which shows temperature profiles for different carbon mass fractions⁵. For $X_c = 0.1$, almost all of the 10^{42} erg released leaves from the surface, since neutrino emission is not important at the lower peak temperature. The recurrence time is 3 years for $y = 10^{12} \text{ g cm}^{-2}$.

Superburst sources have a small range of $M_{\text{Edd}} = 0.1\text{--}0.25 M_{\text{Edd}}$ (Kuulkers, this volume). Cumming & Bildsten [17] showed that for $M_{\text{Edd}} = 0.1 M_{\text{Edd}}$, the carbon burns stably before reach-

⁵ I take $M_{\text{Edd}} = 0.1 M_{\text{Edd}}$, and assume the heating of the layer is by a flux from below of 0.1 MeV per nucleon. Brown [7] has recently emphasised that the flux from below is very sensitive to the thermal conductivity and superfluid properties of the crust [6], so that (unless the carbon layer has an internal heat source) this may be a promising way to constrain the thermal state of the interior.

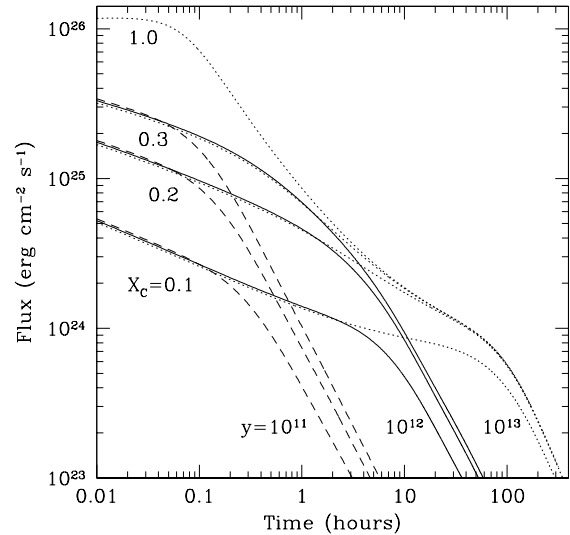


Figure 6. Surface flux against time for cooling models for superbursts (Cumming & Mouchet, in preparation). X_c is the carbon mass fraction, y is the layer column depth (g cm^{-2}).

ing the ignition curve, explaining the lack of superbursts at low rates. Another possibility is that this is related directly to the change in Type I burst behavior observed at $L_x \sim 2 \times 10^{37} \text{ erg s}^{-1}$ in bursters such as K S 1731-260 ($\times 3.3$; [14]). Below the transition, where the accreted fuel burns in regular Type I bursts, the carbon yield is likely very low; above, where the bursts are short and irregular and not burning all the fuel, stable burning could produce significant amounts of carbon. An observational test is to compare bursts in sources with and without superbursts. The regular burster GS 1826-24 should not show a superburst in this picture. For $M_{\text{Edd}} \sim 0.3 M_{\text{Edd}}$, carbon ashes should still occur, but will be less energetic, and show less contrast with the accretion luminosity [17]. Long duration 10^{41} erg bursts are seen from the high M_{Edd} source GX 17+2 [31], but may be too frequent to be carbon ashes [17].

4.2. Time-evolution of the superburst

A simple model of the superburst lightcurve is to assume the carbon burns instantaneously,

without significant vertical mixing. This may be a reasonable assumption since the burning occurs much more rapidly than the convective turnover time (opposite to normal Type I bursts). The thermal evolution of the layer can then be followed as it cools, by evolving the entropy equation in time (Cumming & Macbeth, in preparation). Figure 6 shows a series of lightcurves for different layer thickness (column depth y) and carbon fractions X_C ⁶.

At early times, as the outer parts of the layer thermally adjust, the radiative flux depends mostly on carbon fraction. At late times, after the cooling wave reaches the base of the layer, the flux falls off more steeply. A toy analytic model of the late time cooling is to take a slab with constant thermal diffusivity κ , and perturb the temperature close to the surface, for example at a depth a . For a delta-function perturbation initially, the temperature evolution is given by the Green's function for this case, and the surface flux is $F / \exp(-t/a^2) = t^{-3/2}$, where τ is the thermal time at the initial heating depth $a^2 = \kappa \tau$. At late times, the flux decays as a power law $F / t^{-3/2}$, close to the value found numerically.

For y in the range 10^{12} – 10^{13} g cm⁻² and $X_C = 0.1$ – 0.3 , we find that 10^{42} ergs is radiated from the surface in the first several hours. The observed lightcurves agree well with these cooling models; a more detailed comparison is in progress to see whether X_C and y can be constrained.

The calculations shown in Figure 6 assume that carbon burns to iron group after ignition, giving an energy release of ~ 1 MeV per nucleon. However, Schatz et al. [44] showed that additional energy is released by photodisintegration of elements heavier than iron into iron group nuclei. The binding energy released in going from these heavy nuclei into iron is ~ 0.1 MeV per nucleon, ten times less than carbon burning into iron, but for $X_C \sim 10\%$, this contribution dominates the energetics. This is an interesting additional way in which the nucleimade in the rp process directly

⁶In reality, y and X_C are related by the ignition conditions, but for simplicity we treat y and X_C as free parameters | this also gives a model independent approach in which X_C is just a measure of the deposited energy. For a similar approach see [18].

affect the superburst energetics.

4.3. Interaction between normal Type I bursts and superbursts

Type I bursts disappear (are "quenched") for weeks following the superburst. Cumming & Bildsten [17] proposed that the cooling flux from the superburst stabilizes the hydrogen and helium burning. Assuming an exponential cooling law, they estimated a quenching time of $\sim 5t_{\text{cool}}$ days, where t_{cool} is the cooling time for the layer. This is a little shorter than the observed timescales of weeks (Kuulkers, this volume). However, the cooling models in Figure 6 show a slow power law decay, $F / t^{-3/2}$, at late times rather than exponential. Inspection of Figure 6 shows that the flux reaches 10^{24} erg cm⁻² s⁻¹ in a time ~ 10 h ($y=10^{12}$ g cm⁻²), followed by a $t^{-3/2}$ decay. Assuming the stabilizing flux is 10^{22} erg cm⁻² s⁻¹ [38,3] gives a quenching time

$$t_{\text{quench}} \sim 22 t_{\text{cool}} \sim 9 \text{ days} \frac{y}{10^{12} \text{ g cm}^{-2}}; \quad (3)$$

consistent with observed timescales. Turning this around, a measurement of the quenching time allows the thickness of the layer to be determined.

Whenever the rise of the superburst has been seen, there is a precursor event that resembles a normal Type I burst. A likely explanation for this is that flux from deep carbon burning heats and ignites the layer of H/He accumulating on the surface. This scenario has yet to be investigated in detail, and in particular outstanding questions are the relative timing between precursor and superburst, and whether the vertical propagation of the burning during the rise triggers the precursor. However, simple predictions of this model are: (i) most superbursts should have a precursor (but not all, since a small fraction of the time the helium layer will be too thin to unstably ignite), (ii) a thicker helium layer will ignite with a lower flux, perhaps giving a correlation between precursor energy and the time until the superburst rise, and (iii) the precursor should be weaker than Type I bursts at the same M , since the mass of the H/He layer is less than the critical mass.

The final point is that simultaneous modelling of normal Type I bursts and superbursts gives

an important additional constraint on the models of both [15]. For example, Strohmayer and Brown found a recurrence time of 13 years in their models of the superburst from 4U 1820-30 [49], in which they inferred the accretion rate from the X-ray luminosity. However, using the regular Type I bursting to calibrate the accretion rate gives a shorter recurrence time, 1.2 years for pure helium, 5.10 years for 10% hydrogen [15].

5. CONCLUSIONS

The basic theory of nuclear burning on accreting neutron stars (first outlined over twenty years ago, e.g. [21]) has mixed success in explaining observed Type I X-ray burst properties. The extremely regular burster GS 1826-24 shows remarkable agreement with models of mixed H/He bursts. The observed variation of τ with M strongly suggests that the accreted material has solar metallicity [24]. Regular burst sequences from 4U 1820-30 agree well with accretion and burning of helium-rich matter. For this system, observations of burst sequence variations with recurrence time would constrain the amount of hydrogen present in the accreted material [15], relevant for testing evolutionary models.

Superbursts fit naturally into the picture as ignition of fuel at a much larger depth than normal Type I bursts. Calculations of H/He burning show that the heavy ashes contain a small amount of carbon ($\sim 1\%$). Ignition calculations show that this mixture will unstably ignite giving rise to a burst with properties matching observed properties of superbursts. Time dependent models of the superburst lightcurve show good agreement with the observed exponential decay times and energies. Because stable burning produces more carbon than unstable burning [46], a self-consistent model of carbon production and ignition may require understanding the nature of H/He burning at high accretion rates where bursts are irregular and fuel burns between bursts. There is much to be learned from the interactions between superbursts and normal Type I bursts. The properties of precursors and the time of cessation of bursting after a superburst will tell us much about the underlying layers.

The global Type I bursting behavior remains the biggest puzzle, and may well need new physics to explain it. Another intriguing problem is how to explain bursts with ten minute recurrence times (e.g. see [25]), not predicted by theory. There are many observational constraints which will allow progress to be made: variations of burst properties with accretion rate, shape of burst lightcurves, interactions between normal Type I bursts and superbursts, and the properties of burst oscillations. We are slowly learning more about bursts at higher or lower luminosities than traditional bursters (e.g. [13,31]). Understanding the rich phenomenology of bursts promises to teach us much about these neutron stars and the physical processes in their outer layers.

I thank L. Bildsten, R. Comelisse, D. Galloway, E. Kuulkers, and J. Macbeth for comments on the manuscript. D. Galloway and A. Heger kindly provided data for Fig. 3. I acknowledge support from NASA through Hubble Fellowship grant HF-01138 awarded by the Space Telescope Science Institute, which is operated by the Association of Universities for Research in Astronomy, Inc., for NASA, under contract NAS 5-26555.

REFERENCES

1. Bailyn, C. D. & Grindlay, J. E. 1987, ApJ, 316, L25
2. Basinska, E. M. et al. 1984, ApJ, 281, 337
3. Bildsten, L. 1995, ApJ, 438, 852
4. Bildsten, L. 1998, in *The Many Faces of Neutron Stars*, ed. R. Buccheri, J. van Paradijs, & M. A. A. Par (Dordrecht: Kluwer), 419
5. Bildsten, L. 2000, in *Cosmic Explosions*, the 10th Annual October Astrophysics Conference, Maryland, October 11-13 1999, AIP Conf. 522, ed. S. Holt & W. Zhang (Woodbury NY: AIP)
6. Brown, E. F. 2000, ApJ, 531, 988
7. Brown, E. F. 2003, talk at the "Neutron Stars on Fire" workshop, Princeton, May 2003 (<http://www.sns.ias.edu/burst/>)
8. Brown, E. F. & Bildsten, L. 1998, ApJ, 496, 915
9. Chakrabarty, D., et al. 2003, Nature, 424, 42
10. Chou, Y., & Grindlay, J. E. 2001, ApJ, 563,

- 934
11. Clark, G. W. et al. 1976, *ApJ*, 207, L105
 12. Clark, G. W. et al. 1977, *MNRAS*, 179, 651
 13. Comelisse, R. et al. 2002, *A & A*, 392, 931
 14. Comelisse, R. et al. 2003, *A & A*, 405, 1033
 15. Cumming, A. 2003, *ApJ*, in press (astro-ph/0306245)
 16. Cumming, A., & Bildsten, L. 2000, *ApJ*, 544, 453
 17. Cumming, A., & Bildsten, L. 2001, *ApJ*, 559, L127
 18. Eichler, D. & Cheng, A. F. 1989, *ApJ*, 336, 360
 19. Fedorova, A. V., & Ergma, E. V. 1989, *ApSS*, 151, 125
 20. Franco, L. M. 2001, *ApJ*, 554, 340
 21. Fujimoto, M. Y., Hanawa, T., & Miyaji, S. 1981, *ApJ*, 247, 267
 22. Fujimoto, M. Y., Sztajno, M., Lewin, W. H. G., & van Paradijs, J. 1987, *ApJ*, 319, 902
 23. Fushiki, I. & Lamb, D. Q. 1987, *ApJ*, 317, 368
 24. Galloway, D. K. et al. 2003, *ApJ*, submitted (astro-ph/0308122)
 25. Gottwald, M., Haberl, F., Pamar, A. N., & White, N. E. 1986, *ApJ*, 308, 213
 26. Haberl, F., Stella, L., & White, N. E. 1987, *ApJ*, 314, 266
 27. Hanawa, T. & Fujimoto, M. Y. 1984, *PA SJ*, 36, 199
 28. Hansen, C. J. & van Horn, H. M. 1975, *ApJ*, 195, 735
 29. Hoyle, R., & Fowler, W. A. 1965, in *Quasi-Stellar Sources and Gravitational Collapse*, ed. I. Robinson, A. Schild, & E. L. Shucking (Chicago: University of Chicago Press)
 30. Kuulkers, E. et al. 2002, *A & A*, 382, 503
 31. Kuulkers, E. et al. 2002, *A & A*, 382, 947
 32. Kuulkers, E. et al. 2003, *A & A*, 399, 663
 33. Lamb, D. Q. & Lamb, F. K. 1978, *ApJ*, 220, 291
 34. Lewin, W. H. G., van Paradijs, J., & Taam, R. E. 1995, in *X-Ray Binaries*, ed. W. H. G. Lewin, J. van Paradijs, & E. P. J. van den Heuvel (Cambridge: CUP), 175
 35. Muno, M. P., Fox, D. W., Morgan, E. H., & Bildsten, L. 2000, *ApJ*, 542, 1016
 36. Muno, M. P., Chakrabarty, D., Galloway, D. K., & Savov, P. 2001, *ApJ*, 553, L157
 37. Narayan, R., & Heyl, J. S. 2003, *ApJ*, in press (astro-ph/0303447)
 38. Paczynski, B. 1983, *ApJ*, 264, 282
 39. Podsiadlowski, Ph., Rappaport, S., & Pfahl, E. D. 2002, *ApJ*, 565, 1107
 40. Priedhorsky, W., & Terrell, J. 1984, *ApJ*, 284, L17
 41. Rasio, F. A., Pfahl, E. D., & Rappaport, S. 2000, *ApJ*, 532, L47
 42. Schatz, H. et al. 1998, *Phys. Rep.*, 294, 167
 43. Schatz, H. et al. 2001, *PRL*, 86, 3471
 44. Schatz, H., Bildsten, L., & Cumming, A. 2003, *ApJ*, 583, L87
 45. Schatz, H., Bildsten, L., Cumming, A., & Wiescher, M. 1999, *ApJ*, 524, 1014
 46. Schatz, H., Bildsten, L., Cumming, A., & Ouellette, M. 2003, *Nuclear Physics A*, 718, 247
 47. Stella, L., Priedhorsky, W., & White, N. E. 1987, *ApJ*, 312, L17
 48. Strohmayer, T. E., & Bildsten, L. 2003, in *Compact Stellar X-Ray Sources*, eds. W. H. G. Lewin and M. van der Klis (Cambridge: Cambridge University Press) (astro-ph/0301544)
 49. Strohmayer, T. E., & Brown, E. F., 2002, *ApJ*, 566, 1045
 50. Taam, R. E. & Picklum, R. E. 1978, *ApJ*, 224, 210
 51. Taam, R. E. 1980, *ApJ*, 241, 358
 52. Tutukov, A. V., Fedorova, A. V., Ergma, E. V., & Yungelson, L. R. 1987, *Sov. Astron. Lett.*, 13, 328
 53. Ubertini, P., et al. 1999, *ApJ*, 514, L27
 54. van Straaten, S., van der Klis, M., Kuulkers, E., & Mendez, M. 2001, *ApJ*, 551, 907
 55. Verbunt, F. 1987, *ApJ*, 312, L23
 56. van Paradijs, J., Penninx, W., & Lewin, W. H. G. 1988, *MNRAS*, 233, 437
 57. Wallace, R. K. & Woosley, S. E. 1981, *ApJS*, 45, 389
 58. Wallace, R. K. & Woosley, S. E. 1984, *High Energy Transients in Astrophysics*, 319
 59. Wijands, R. 2001, *ApJ*, 554, L59
 60. Woosley, S. E. et al. 2003, *ApJ*, submitted (astro-ph/0307425)
 61. Woosley, S. E. & Taam, R. E. 1976, *Nature*, 263, 101